Catalysis Communications 35 (2013) 11–16

Contents lists available at SciVerse ScienceDirect

Catalysis Communications

journal homepage: www.elsevier.com/locate/catcom

Short Communication

Palladium supported on zinc ferrite: A highly active, magnetically separable catalyst for ligand free Suzuki and Heck coupling

Abhilash S. Singh, Umakant B. Patil, Jayashree M. Nagarkar *

Department of Chemistry, Institute of Chemical Technology, Matunga, Mumbai, 400019, India

ARTICLE INFO

Article history:
Received 24 November 2012
Received in revised form 5 February 2013
Accepted 7 February 2013
Available online 15 February 2013

Keywords:
Magnetic nanoparticle
Pd–zinc ferrite
Heterogeneous catalyst
Co-precipitation
C – C coupling reaction

ABSTRACT

An efficient superparamagnetic solid catalyst has been synthesized by loading Pd(0) species during synthesis of zinc ferrite nanoparticles by ultrasound assisted co-precipitation in the absence of surface stabilizer or capping agent. Various techniques were employed to characterize the as-synthesized Pd–$ZnFe_2O_4$ magnetic nanoparticles. The catalyst showed excellent performance for Suzuki and Heck coupling reactions under ligand free condition. The catalyst being super paramagnetic was separated by using an external magnet and reused for five cycles without any appreciable loss in the activity.

1. Introduction

In recent years, for environmentally benign chemical methodologies magnetic nano materials have emerged as alternatives to usual heterogeneous supports [1,2]. Metal nanoparticles dispersed on the surface of an oxide works as an efficient catalyst for a wide variety of reactions as compared to bulk particles [3,4]. Palladium catalyzed Suzuki and Heck coupling reactions are widely used methods for the formation of C – C bonds [5,6]. Generally these coupling reactions were studied by using homogeneous catalyst of palladium complex with various ligands such as phosphines [7], dibenzylideneacetone (dba) [8] and carbenes [9]. The palladium compounds are also used in homogeneous catalysis under ligand free condition [10,11]. However the high cost of palladium complexes and difficulties in product separation makes the process tedious [12]. A variety of materials such as carbon [13], clay [14], metal oxide [15], silica [16], zeolite [17] and polymer resin [18] were also developed as support for nanoparticles.

Magnetic nanoparticles (MNPs) have been effectively employed as catalyst support for various organic transformations [19]. They serve as support for the metal and as an alternative to filtration thereby preventing loss of catalyst [20,21]. The thermal stability and the catalytic activity of the palladium catalyst were profoundly increased by supporting it on magnetic nanoparticles [22,23]. Magnetically separable Pd-based catalysts have been well reported for coupling reactions [24–27]. Palladium loaded on magnetic support is most essential heterogeneous catalyst as they offered high surface area and easy catalyst separation. However, most of the processes require tedious procedure to anchor the active palladium species on the magnetic support surfaces. Herein we report successful loading of Pd(0) species on super paramagnetic zinc ferrite without using organic capping agent or surface stabilizer under ultrasonic irradiation. The catalytic activity and stability of the palladium nano catalyst was tested by selecting Suzuki and Heck coupling as the model reactions. The catalyst was found to be highly efficient, recyclable, and environmentally friendly.

2. Experimental section

2.1. Synthesis of palladium nanoparticles and its surface adsorption on $ZnFe_2O_4$ magnetic nanoparticles

Pd NPs were synthesized by using poly(ethyleneglycol) (PEG) and $Pd(OAc)_2$ as precursors [28] (see supplementary data).

2.2. Material characterization

The prepared catalyst was characterized by various techniques such as SEM, TEM, XRD, FTIR, BET, DSC and TGA. Powder X-ray diffraction (PXRD) pattern was recorded on a PANalytical MPD diffractometer using Cu Kα radiation ($\lambda = 1.5406$ A°) at 40 kV and 40 mA. Transmission electron microscopy (200 kV TEM, JEOL JEM2100) was used to examine morphology and size of the nano particles. Scanning electron micrographs (SEM) and Energy dispersive X-ray Analysis (EDAX) analysis were recorded on a single instrument FEI Quanta 200 ESEM FEG. The IR spectrum was recorded using FT-IR spectrophotometer (Perkin Elmer Spectrum 100) as KBr pellets. The UV–vis analysis was performed using a (Uv-1650 Pc Shimadzu). The BET analysis was performed by

---

* Corresponding author. Tel.: +91 22 33611111/2222; fax: +91 22 33611020.
E-mail addresses: jm.nagarkar@ictmumbai.edu.in, jayashreenagarkar@yahoo.co.in (J.M. Nagarkar).

1566-7367/$ – see front matter © 2013 Elsevier B.V. All rights reserved.
http://dx.doi.org/10.1016/j.catcom.2013.02.003

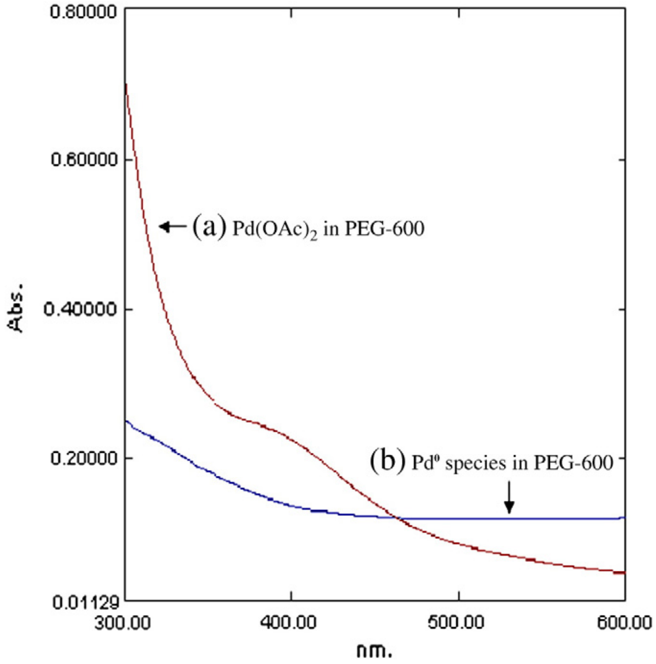

Fig. 1. UV–vis spectra of (a) $Pd(OAc)_2$ in PEG-600 (b) Pd(0) species in PEG-600.

nitrogen adsorption–desorption method at liquid N_2 temperature (Micromeritics-ASAP 2020). Differential scanning calorimetric and thermogravimetric (DSC/TG) analysis were carried by using Mettler Toledo instrument under N_2 atmosphere. The yield of products has been determined by GC (PerkinElmer Clarus 400). Purity of all compounds was determined with the help of GC–MS analysis (Shimadzu QP-2010). Magnetic measurements of the powder samples were determined by using vibrating-sample magnetometer (PPMS Quantum Design Inc.).

2.3. General procedure for Suzuki and Heck reaction

The determined parameters for Suzuki cross-coupling reaction consists of 0.5 mmol aryl halide in 5 mL of pure ethanol, 0.75 mmol phenyl boronic acid, 1.5 mmol K_2CO_3 and 8 mg Pd–$ZnFe_2O_4$ catalyst (4.62 mol%). The reaction was carried under reflux condition for 3–9 h and monitored by Gas Chromatography (GC). The reaction mixture was cooled to room temperature after completion and the catalyst (MNPs) was separated using an external magnet. The catalyst was then washed with ethanol, dried at 100 °C for 3 h and preserved for next run. Similarly for Heck cross-coupling reactions 0.5 mmol aryl halide in 5 mL DMF, (1.0 mmol) methyl acrylate or styrene (1.5 mmol), Et_3N (1.5 mmol), and 4.62 mol% catalyst (0.12 mol% of Pd) were added together. The reaction mass was heated at 120 °C for specific time. The separation and regeneration of catalyst were similar to Suzuki reaction.

3. Results and discussion

3.1. Characterization of the Pd incorporated $ZnFe_2O_4$ MNPs

The formation of Pd(0) species was observed from UV–vis spectrophotometric measurement (300–600 nm) as shown in Fig. 1. The total disappearance of peak at 400 nm in the UV–vis spectrum indicates the complete conversion of Pd (II) to Pd(0) species.

The $ZnFe_2O_4$ MNPs were synthesized in high yield by using sonochemical co-precipitation technique in aqueous medium without additional surfactant or organic capping agent. The elemental composition of the dark brown particles was confirmed using EDAX analysis as depicted in Fig. 2. The distribution of the elements in the Pd incorporated $ZnFe_2O_4$ was Zn = 11.52%, Fe = 23.62%, O = 64.05% and Pd = 0.81%. The ratio of iron/zinc in $ZnFe_2O_4$ was found to be 2.05 which are in very good agreement with the theoretical value of 2.0.

Fig. 3 depicts the powder X-ray diffraction pattern of the Pd- $ZnFe_2O_4$ MNPs catalyst and represents similarity with the characteristic reflections of cubic phase thereby confirming the structural purity of the sample. Since the concentration of palladium is very low, its characteristic XRD peaks (200), (220) and (111) cannot be seen in the XRD pattern of the catalyst. However broadened (111) diffraction peaks can be still identified in PXRD pattern. The crystallite size for the nanoparticles was based on X-ray diffraction line broadening and calculated by using Scherrer equation [29]. It was found to be 10 ± 5 nm which was in good agreement with the particle size obtained from TEM micrographs.

Furthermore, the morphology of the Pd–$ZnFe_2O_4$ MNPs was investigated using SEM and TEM and the images are shown in Figs. 4 and 5, respectively. The TEM image of the catalyst was also obtained after the fifth cycles. There was no significant change in the morphology

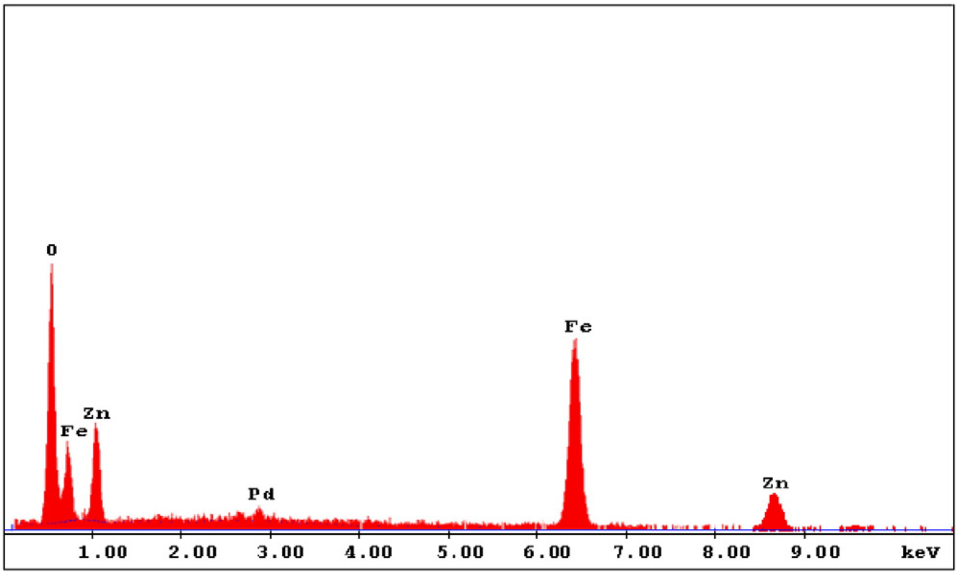

Fig. 2. EDX analysis of Pd–$ZnFe_2O_4$ MNPs.

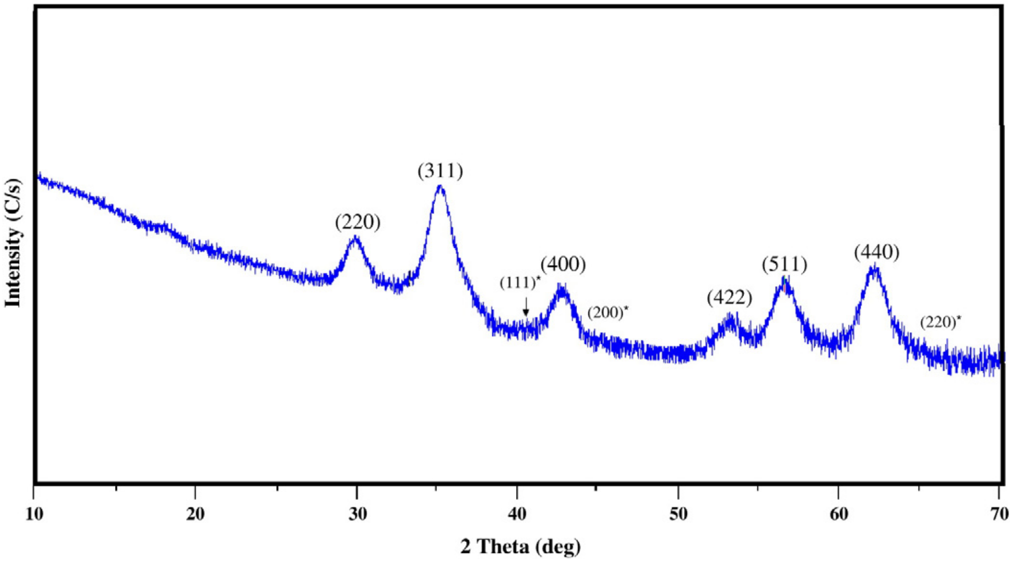

Fig. 3. PXRD pattern of Pd–$ZnFe_2O_4$ MNPs (* contribution from Pd NPs).

and dispersion of the particles. TEM images of the catalyst at different magnifications were also recorded (Supporting Information Fig. 1).

From the N_2 adsorption–desorption isotherm of Pd–$ZnFe_2O_4$ MNPs, the BET surface area of the particles was found to be 76 m^2/g (Supporting Information Fig. 5). The adsorption average pore width is 241A°. The single point surface area at $P/Po = 0.2551$ is 75 m^2/g.

The surface of the catalyst was further examined with the help of FT-IR spectra (Supporting Information Fig. 2). The IR spectrum shows two absorption peaks at 3420 cm^{-1} and 1620 cm^{-1} due to the surface adsorbed water with other characteristic peak of cubic ferrite. The moisture content of the catalyst was determined by Karlfischer Titrator and it was found to be 0.01%w/w. The magnetic properties of the as prepared Pd–$ZnFe_2O_4$ MNPs were investigated by PPMS. The room temperature magnetization curve of the catalyst represents very low coercive force with no apparent hysteresis curve signifying a superparamagnetic quality of the catalyst (Supporting Information Fig. 6). The magnetic oxide nanoparticles with a size of 30–40 nm or less than that are single-domain and illustrate superparamagnetic behavior [30].

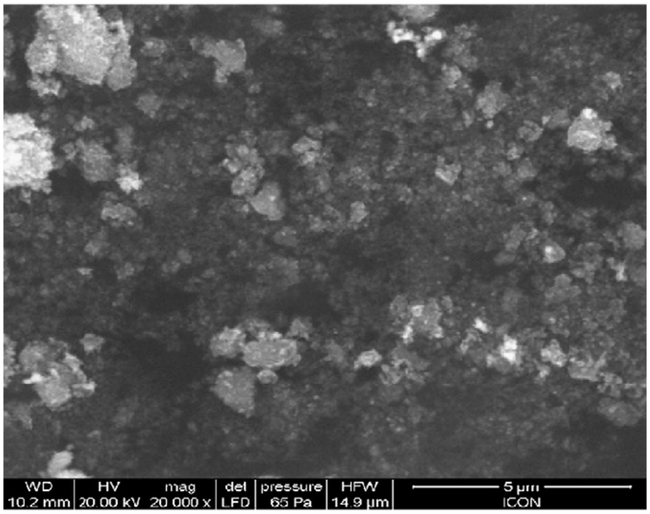

Fig. 4. SEM image of Pd–$ZnFe_2O_4$ MNPs.

3.2. Catalytic activity of the as-synthesized nano particles

The catalytic activity of the as-synthesized Pd–$ZnFe_2O_4$ MNPs was evaluated for both Suzuki (Scheme 1) and Heck (Scheme 2) reactions.

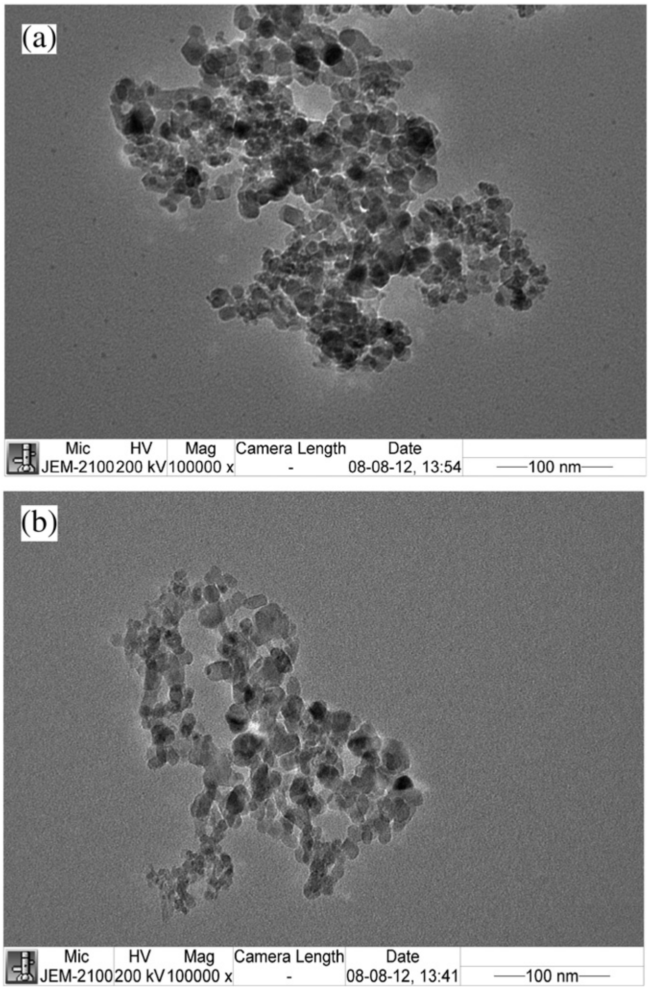

Fig. 5. TEM images of the Pd–$ZnFe_2O_4$ (a) before reaction (b) after five cycles of Suzuki reactions.

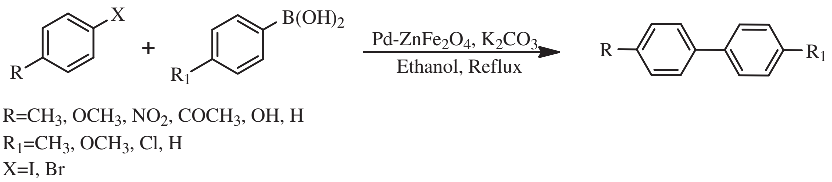

Scheme 1. Suzuki cross coupling reaction of aryl halides with phenylboronic acid.

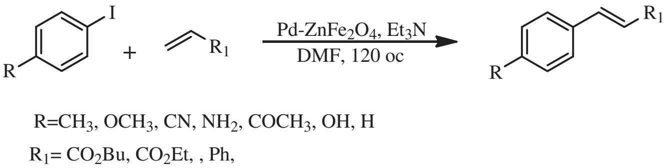

Scheme 2. Heck reaction of aryl halides and alkenes.

The reactions were carried out with different solvents, bases and at different temperatures to obtain the optimized reaction conditions (supporting information). No product is formed when zinc ferrite is used in the absence of palladium. The TON and TOF for Suzuki reaction i.e. coupling of iodobenzene and phenylboronic acid was found to be 2168 and 542 h^{-1}. Similarly the TON and TOF for Heck reaction (coupling of iodobenzene and ethylacrylate) was 2168 and 1084 h^{-1}.

Suzuki reaction was studied for wide variety of aryl halides and boronic acids under optimized conditions. The scope of the catalyst was tested by using various electron-rich and electron-deficient substrates (Table 1). No homocoupled product is formed when the yield is less. The catalyst was separated by using external magnet. The reaction mixture was then separated by decantation. Thereafter, the flask was washed with ethanol and combined organic layer was dried over anhydrous sodium sulfate and evaporated in a rotary evaporator under reduced pressure followed by column chromatography to obtain the pure product.

The application of Pd–$ZnFe_2O_4$ MNPs was also investigated for Heck reaction. The reaction was optimized for the best conditions (supporting information).

The scope of the catalyst for Heck reaction was studied for wide variety of aryl halides with various alkenes (Scheme 2, Table 2). The catalyst failed to catalyze the reaction of aryl chlorides. The catalyst separation and recyclability procedures are similar to Suzuki reactions. The recyclability of the catalyst was estimated using a Suzuki reaction of 4-methoxyiodobenzene and phenylboronic acid. Heck reaction was carried out between iodobenzene and ethylacrylate. The activity of Pd–

Table 1
Suzuki reaction of various aryl halides with phenylboronic acid catalyzed by Pd–$ZnFe_2O_4$ MNP.[a]

Entry	Aryl halide	Boronic acid	Product(s)	Time (h)	Yield (%)[b]
1	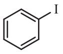	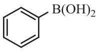	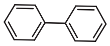	4 h	92
2	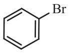	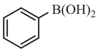	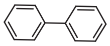	9 h	85
3	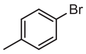	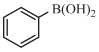	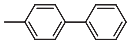	9 h	89
4	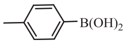	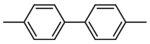	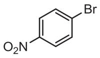	9 h	91
5	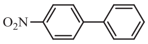	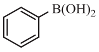	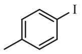	8 h	90
6	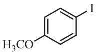	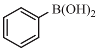	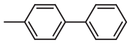	3.5 h	91
7	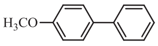	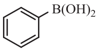	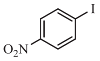	3 h	90
8	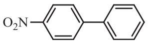	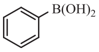	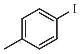	3.5 h	94
9	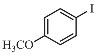	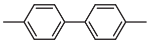	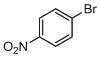	3.5 h	91
10	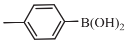	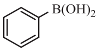	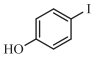	4 h	95
11	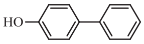	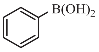	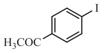	3.5 h	91
12	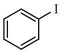	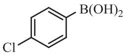	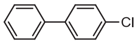	4 h	93
13	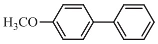	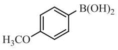	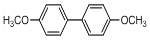	3 h	92
14	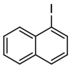	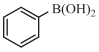	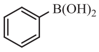	4 h	92
15	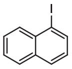	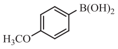	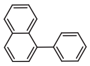	3.5 h	92

[a] Reaction condition: 0.5 mmol of aryl halide, 0.75 mmol of boronic acid, 1.5 mmol of K_2CO_3, 4.62 mol% of Pd–$ZnFe_2O_4$ MNPs and 5 mL ethanol, reflux.

[b] Isolated yield by column chromatography.

Table 2
Heck reaction of various aryl halides with alkenes catalyzed by Pd–$ZnFe_2O_4$ MNP.[a]

Entry	Aryl halide	Alkenes	Product(s)	Time (h)	Yield (%)[b]
1	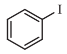	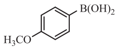	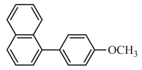	2 h	96
2	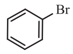	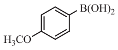	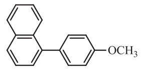	6 h	88
3	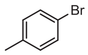	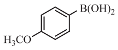	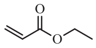	6 h	90
4	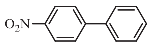	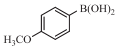	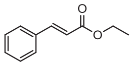	5 h	92
5	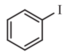	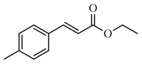	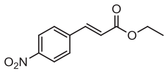	2 h	94
6	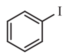	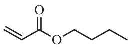	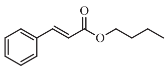	3 h	90
7	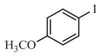	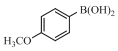	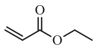	2 h	96
8	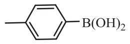	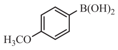	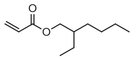	4 h	89
9	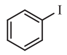	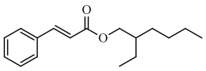	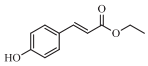	6 h	94
10	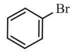	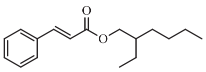	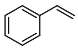	12 h	65
11	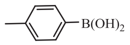	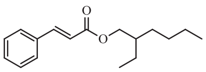	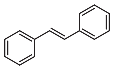	12 h	80
12	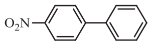	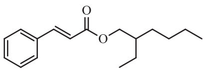	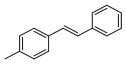	12 h	90
13	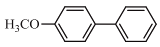	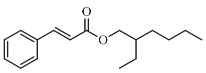	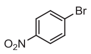	6 h	95
14	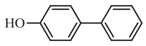	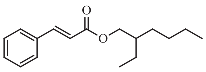	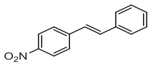	6 h	90
15	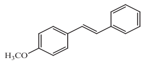	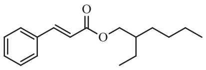	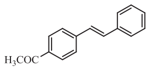	12 h	82
16	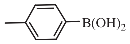	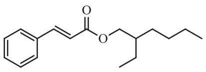	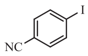	14 h	80
17	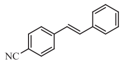	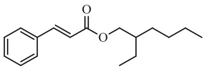	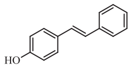	10 h	85

[a] Reaction condition: Iodobenzene (0.5 mmol), alkenes (1 mmol), Et_3N (1.5 mmol), DMF (5 mL), 120 °C and 4.62 mol% of Pd–$ZnFe_2O_4$ MNPs.
[b] Isolated yield based on column chromatography.

$ZnFe_2O_4$ MNP catalyst is shown in Table 3. The amounts of Pd leaching into solution for the Suzuki and Heck coupling reactions were determined through ICP-AES.

In Suzuki reaction, no deactivation of catalyst was found till third cycle and after fifth cycle the Pd loss was found to be 0.5 wt.% of total Pd content. The average Pd loss for the Heck reaction was 4.2 wt.% of total Pd content. If the Suzuki reaction is performed in a condition similar to Heck reaction the leaching is almost similar, due to high reaction temperature and solvent, but the product yield is only 20%. The hot filtration test after 1 h gave 0% conversion for Suzuki and 2% conversion for Heck after continuing the reaction for 24 h, indicating negligible palladium leaching and heterogeneity of the catalyst. The ICP-MS elemental analysis of the colored solution shows the palladium concentration of 17 ppb for Suzuki reaction and 25 ppb for Heck reaction. This loss in Pd content explains the decrease in yield with increase in the number of recycle runs.

Table 3
Activity of Pd–$ZnFe_2O_4$ MNP for Suzuki and Heck reactions.

	Recycle runs	Conversion (%)	TOF (h^{-1})[c]
Suzuki reaction[a]	1st	100	542
	2nd	100	542
	3rd	99	528
	4th	99	528
	5th	98	516
Heck reaction[b]	1st	100	1084
	2nd	100	1084
	3rd	99	1073
	4th	98	1062
	5th	97	1051

[a] Reaction conditions: 4-$IPhOCH_3$, $PhB(OH)_2$, K_2CO_3, Ethanol, catalyst 8 mg of Pd–$ZnFe_2O_4$ and temp = reflux and time = 3 h.
[b] Reaction conditions: PhI, ethylacrylate, Et_3N, DMF, catalyst 8 mg of Pd–$ZnFe_2O_4$, Temp = 120 °C and time = 2 h.
[c] TOF = mol product/mol catalyst ($\times h^{-1}$).

4. Conclusion

In conclusion, we have developed a highly efficient magnetic catalyst of Pd incorporated $ZnFe_2O_4$, suitable for Suzuki and Heck cross-coupling reactions. The reactions can be carried out under ligand free and aerobic conditions with low catalyst loading. The catalyst was easily recovered by magnetic separation and showed high catalytic activity. Hence, Pd–$ZnFe_2O_4$ catalyst can be considered as another interesting example in heterogeneous catalysis.

Acknowledgments

Financial support from Green Tech. U.P.E. is gratefully acknowledged.

Appendix A. Supplementary data

Supplementary data to this article can be found online at http://dx.doi.org/10.1016/j.catcom.2013.02.003.

References

[1] R. Abu-Reziq, H. Alper, D. Wang, M.L. Post, Journal of the American Chemical Society 128 (2006) 5279–5282.
[2] S. Shylesh, V. Schunemann, W.R. Thiel, Angewandte Chemie International Edition 49 (2010) 3428–3459.
[3] A. Cao, G. Veser, Nature Materials 9 (2010) 75–81.
[4] C.T. Campbell, S.C. Parker, D.E. Starr, Science 298 (2002) 811–814.
[5] N. Miyaura, A. Suzuki, Chemical Reviews 95 (1995) 2457–2483.
[6] R.F. Heck, Palladium Reagents in Organic Synthesis, Academic Press, London, 1985.
[7] C.A. Fleckenstein, H. Plenio, Chemical Society Reviews 39 (2010) 694–711.
[8] C. Amatore, A. Jutand, Coordination Chemistry Reviews 178 (1998) 511–528.
[9] N. Marion, S.P. Nolan, Accounts of Chemical Research 41 (2008) 1440–1449.
[10] G.W. Kabalka, V. Namboodiri, L. Wang, Chemical Communications (2001) 775.
[11] M. Mondal, U. Bora, Green Chemistry 14 (2012) 1873–1876.
[12] X. Liu, A. Wang, X. Yang, T. Zhang, C.Y. Mou, D.S. Su, J. Li, Chemistry of Materials 21 (2009) 410–418.
[13] F.X. Felpin, T. Ayad, S. Mitra, European Journal of Organic Chemistry 12 (2006) 2679–2690.
[14] B.M. Choudary, S. Madhi, N.S. Chowdari, M.L. Kantam, B. Sreedhar, Journal of the American Chemical Society 124 (2002) 14127–14136.
[15] Y. Yamada, C.K. Tsung, W. Huang, Z. Huo, S.E. Habas, T. Soejima, C.E. Aliaga, G.A. Somorjai, P. Yang, Nature Chemistry 3 (2011) 372.
[16] C.H. Tu, A.Q. Wang, M.Y. Zheng, X.D. Wang, T. Zhang, Applied Catalysis A 297 (2006) 40–47.
[17] S. Mandal, D. Roy, R.V. Chaudhari, M. Sastry, Chemistry of Materials 16 (2004) 3714–3724.
[18] R.S. Underhill, G. Liu, Chemistry of Materials 12 (2000) 3633–3641.
[19] C.W. Lim, I.S. Lee, Nano Today 5 (2010) 412–434.
[20] J. Ge, Q. Zhang, T. Zhang, Y. Yin, Angewandte Chemie International Edition 47 (2008) 8924–8928.
[21] Y. Deng, Y. Cai, Z. Sun, J. Liu, C. Liu, J. Wei, W. Li, C. Liu, Y. Wang, D. Zhao, Journal of the American Chemical Society 132 (2010) 8466–8473.
[22] V. Polshettiwar, R. Luque, A. Fihri, H. Zhu, M. Bouhrara, J.M. Basset, Chemical Reviews 111 (2011) 3036–3075.
[23] B. Baruwati, D. Guin, S.V. Manorama, Organic Letters 9 (2007) 5377–5380.
[24] M. Zhu, G. Diao, Journal of Physical Chemistry C 115 (2011) 24743–24749.
[25] Z. Gao, Y. Feng, F. Cui, Z. Hua, J. Zhou, Y. Zhu, J. Shi, Journal of Molecular Catalysis A: Chemical 336 (2011) 51–57.
[26] K.K. Senapati, S. Roy, C. Borgohain, P. Phukan, Journal of Molecular Catalysis A: Chemical 352 (2012) 128–134.
[27] P. Li, L. Wang, L. Zhang, G.W. Wang, Advanced Synthesis and Catalysis 354 (2012) 1307–1318.
[28] C. Luo, Y. Zhang, Y. Wang, Journal of Molecular Catalysis A: Chemical 229 (2005) 7–12.
[29] B.D. Cullity, Elements of X-ray Diffraction, Addision-Wesely, London, 1959, pp. 261–262.
[30] M. Niederberge, N. Pinna, Metal Oxide Nanoparticles in Organic Solvents: Synthesis Formation, Assembly and Application, Springer, London, 2009, pp. 176–177.